available at www.sciencedirect.com

SCIENCE DIRECT®

journal homepage: www.elsevier.com/locate/biochempharm

Cytosolic heat shock proteins and heme oxygenase-1 are preferentially induced in response to specific and localized intramitochondrial damage by tetrafluoroethylcysteine

Han K. Ho [a,1], *Yankai Jia* [a], *Kevin J. Coe* [a], *Qiuxia Gao* [a], *Catalin E. Doneanu* [a], *Zhonghua Hu* [d], *Theo K. Bammler* [c], *Richard P. Beyer* [c], *Nelson Fausto* [b], *Sam A. Bruschi* [a], *Sidney D. Nelson* [a,*]

[a] *Department of Medicinal Chemistry, University of Washington, Box 357610, Seattle, WA 98195, USA*
[b] *Department of Pathology, University of Washington, Seattle, WA 98195, USA*
[c] *Department of Environmental Health, University of Washington, Seattle, WA 98195, USA*
[d] *Amgen, Inc., Seattle, Washington 98119, USA*

ARTICLE INFO

Article history:
Received 3 February 2006
Accepted 14 March 2006

Keywords:
Tetrafluoroethylcysteine
Heat shock proteins
Microarray
Cytotoxicity
Mitochondrial dysfunction
Heme oxygenase

ABSTRACT

Previously, S-(1,1,2,2-tetrafluoroethyl)-L-cysteine (TFEC) was shown to mediate cytotoxicity by covalently modifying a well-defined group of intramitochondrial proteins including aconitase, α-ketoglutarate dehydrogenase (αKGDH) subunits, heat shock protein 60 (HSP60) and mitochondrial HSP70 (mtHSP70). To investigate the cellular responses to this mitochondrial damage, microarray analysis of TFEC treated murine hepatocytes of the TAMH cell line was carried out. Results of these studies revealed a HSP response that was significantly stronger than other well-characterized hepatotoxicants including acetaminophen, diquat and rotenone. Specifically, cytosolic *HSP25*, *HSP40*, *HSP70*, *HSP105* and microsomal *HSP32* (*HO-1*) were strongly upregulated within the first few hours of TFEC treatment, while little change was observed among other HSPs that are predominantly localized in the mitochondria and endoplasmic reticulum (ER). Post-translational modification of HSP25 was also observed with the appearance of a unique DTT-resistant immunoreactive band at about 50 kDa, a putative dimer. The biological significance of HSP responses to TFEC-induced toxicity were subsequently demonstrated using the "gain of function" pretreatment: heat shock. Overall, we report an atypical HSP induction profile that does not conform to changes expected of a classical temperature shock. Furthermore, despite a well-defined intramitochondrial origin of toxicity, TFEC rapidly evokes an early and strong upregulation of cytosolic stress proteins. The cytoprotective effects of such HSP responses suggest a plausible role in modulating the progression of TFEC-induced cellular injury.

* *Corresponding author*. Tel.: +1 206 543 8503; fax: +1 206 685 3252.
E-mail address: sidnels@u.washington.edu (S.D. Nelson).

[1] Present address: Center for Molecular Medicine, Agency for Science, Technology and Research, Singapore 138673, Singapore.

0006-2952/$ – see front matter © 2006 Elsevier Inc. All rights reserved.
doi:10.1016/j.bcp.2006.03.019

1. Introduction

Mitochondria play an essential role in maintaining cellular survival. For decades, the mitochondrion has been known to be the central organelle for harnessing energy needed for sustaining most biochemical processes. More recently, another dimension to their physiological role has emerged with the discovery of a mitochondrial signaling pathway involved in apoptosis. Members of the BCL-2 family like BAX, BAK and BID, provide important and early triggers for mitochondrial membrane perturbations, resulting in subsequent membrane permeability transition and the release of cytochrome c thereby leading to caspase activation [1,2]. These biochemical changes are ultimately responsible for the morphological aspects of some apoptotic forms of cell death. Clearly, the influence of mitochondria encompasses both ''life and death'' events in most organisms. It is not surprising that dysfunction of this organelle has been implicated in a number of disease states which include Parkinson's, Alzheimer's, cardiomyopathies, as well as a number of drug-induced toxicities [3,4].

Although biochemical pathways affected by mitochondrial dysfunction have been well studied in several systems, there remain many effects that are not completely understood. Even less is known regarding the management of mitochondrially based diseases through possible pharmacological interventions. Thus, we are interested in determining the generalized cellular responses to mitochondrial damage that may help identify potential subcellular targets and signature events that can be exploited for therapies against such pathologies.

Towards this objective, S-(1,1,2,2-tetrafluoroethyl)-L-cysteine (TFEC) was used as a toxicant that elicits a specific intramitochondrial stress. TFEC is an in vivo metabolite of the industrial gas tetrafluoroethylene (widely used as a precursor for TEFLON™ coating) and is generated from the sequential metabolism of the parent compound through the mercapturate pathway [5]. A number of independent studies have demonstrated that TFEC, and tetrafluoroethylene by implication, can result in acute and chronic kidney and liver toxicities [6–9]. TFEC bioactivation occurs as a result of cleavage at the β position by pyridoxal-dependent aminotransferases located in the mitochondria [10,11]. This results in the formation of a highly reactive electrophilic intermediate, difluorothionoacetylfluoride (DFTAF), which readily binds to exposed ε-amino lysine groups on adjacent proteins [7,12]. Cell culture and animal models have been used to demonstrate cytotoxicity after TFEC administration with the reproducible formation of specific covalently modified intramitochondrial proteins. These include mitochondrial enzymes essential for cellular and organism viability such as aconitase, α-ketoglutarate dehydrogenase (KGDH) E2 and E3 subunits, HSP60 and HSP70 [7,13]. Particularly, a cell line that preserves a differentiated hepatocytic phenotype, mouse hepatocytes stably transfected to express transforming growth factor-α (TAMH) [14], was used that demonstrated similar inhibition of aconitase and KGDH to that observed in vivo, as well as the consequent depletion of NADH and ATP biosynthesis after TFEC treatment [7,15].

Therefore, TAMH was used as a model for TFEC-induced cytotoxicity [7,14,16,17]. We report here the early transcriptional and translational changes that accompany and are important in the manifestation and progression of intramitochondrially initiated cytotoxicity.

2. Materials and methods

2.1. Cell culture

Serum-free cell culture of the TAMH line between passages 21–35 was undertaken as previously described [14,17]. All chemicals were obtained from Sigma (St. Louis, MO) unless otherwise stated. Briefly, cells were grown in serum-free Dulbecco's modified Eagle's medium/Ham's F12 (Invitrogen, Carlsbad, CA) supplemented with 5 μg/mL insulin, 5 μg/mL transferrin, 5 ng/mL selenium (Collaborative Biomedical Products, Boston, MA), 100 nM dexamethasone, 10 mM nicotinamide and 0.1% (v/v) gentamicin (Invitrogen). Cultures were maintained in a humidified incubator with 5% carbon dioxide/95% air at 37 °C and passaged at 70–90% confluence.

2.2. RNA isolation

Cells were grown to confluence in 150 cm^2 tissue culture dishes in quadruplicate for each sample, and treated with 200 μM TFEC for 2, 4 and 6 h. At the end of respective treatments, cells were harvested by scraping with a rubber policeman. The resultant cell pellets were spun down and washed once with Dulbecco's PBS (Invitrogen). Immediately, 1 mL of Trizol reagent (Invitrogen) per 10^7 cells was added for cell lysis. After vortexing, the lysate was passed through a 22G needle 10 times to ensure complete lysis. Chloroform (0.2 mL) was rapidly added to every 1 mL of cell lysate and vortexed vigorously for 15 s. Lysate aliquots (1 mL) were measured into microcentrifuge tubes and left to stand for 2–3 min before spinning at 10,000 rpm for 15 min at 4 °C. Gently, 0.5 mL of aqueous phase was transferred to a fresh tube, and an equal volume of 70% ethanol was added. This resulting mix was loaded onto an RNeasy column (Qiagen, Valencia, CA) and purified total RNA was extracted according to the manufacturer's protocol.

2.3. Microarray analysis procedures

Gene expression analyses were performed using the Amersham, Codelink 10K mouse array (Amersham Biosciences, Piscataway, NJ) according to manufacturer's protocols. Briefly, total RNA from each sample was quantified before first and second strand cDNA synthesis. The resulting double-stranded cDNA was purified with a QIAquick spin column (Qiagen). After drying the cDNA in a SpeedVac concentrator, cRNA was synthesized by in vitro transcription and purified using the RNeasy kit (Qiagen). The quality of the cRNA was evaluated using an Agilent 2100 Bioanalyzer (Agilent, Palo Alto, CA) and samples with A260:A280 ratios between 1.8 and 2.1 were used for subsequent microarray analyses. Each 10 μg of cRNA sample was hybridized onto Codelink microarray slides and incubated for 18 h at 37 °C. At the end of incubation, the arrays were washed with 0.75× TNT buffer (0.1 M Tris–HCl pH 7.6, 0.15 M NaCl, 0.05% Tween-20) at 46 °C for 1 h and incubated with streptavidin–Alexa 647 (Molecular Probes, Eugene, OR)

working solution at 25 °C for 30 min to label the fluorogenic probe. The arrays were scanned with an Axon GenePix 4000B fluorescent scanner and the GenePix Pro imaging software (Axon Instruments, Foster City, CA). Fluorescent intensity of each spot in the image was determined using ImaGene™ 5 (Biodiscovery, Marina del Rey, CA) for spot finding and analysis.

2.4. Quantitative RT-PCR

Quantitative RT-PCR was carried out using an ABI Prism 7700 Sequence detection system (Applied Biosystems, Foster City, CA) with SYBR Green dye as the fluorogenic probe. The thermal cycling condition comprised an initial denaturation step at 95 °C for 10 min, followed by 40 cycles at 95 °C for 20 s and 62 °C for 60 s. The gene-specific sequences of the primer pairs and probes used in the assays were as follows: *HSP25* (NM_013560): forward primer, TGTCCCTGGACGTCAACCACTT; reverse primer, ACCTGGAGGGAGCGTGTATTTC. *HO-1* (NM_010442): forward primer, GCACAGGGTGACAGAAGAGGCTA; reverse primer, ATCTGTGAGGGACTCTGGTCTTTGT. *HSP40* (NM_006145): forward primer, GGGACCAGACCTCGAACAACAT; reverse primer, ACCACAGAGAGCCTCCCGAA. *HSP105* (NM_006644): forward primer, GAGGCAAGGATGAGAAATACAACCAC; reverse primer, CAATTCCTTGACCTTCGCTCTGAT. *HSP60* (X53584): forward primer, AAGCTGAACGAGCGACTTGCTAA; reverse primer, GCTGCTCTTGTAGCATTGAGAGCA. *mtHSP70* (NM_010481): forward primer, CAGCGCTCATTGAAACTCTTC; reverse primer, GTGCCAGAACTTCCAGAACCTTC. *HSP70i* (M12573): forward primer, TCCTATGCCTTCAACATGAAGAGC; reverse primer, GAGATGACCTCCTGGCACTTGTC. *GAPDH* (NM_008084): forward primer, TCCTGCACCACCAACTGCTT; reverse primer, GAGGGGCCATCCACAGTCTT.

2.5. Statistical analysis and data normalization

Statistical analyses and data normalization were carried out with Bioconductor software (Harvard University, Boston, MA). The foreground spot intensities from all the bioarrays used were normalized as a group using quantile normalization as described previously [18]. Heat maps of selected HSP expression profiles were generated using GeneSifter software (VizXlabs, Seattle, WA).

2.6. Subcellular fraction isolation

Mitochondria-enriched fractions were isolated with slight modifications to the protocol described previously [19]. Briefly, the harvested cells were pelleted using a bench top microcentrifuge. Supernatant was removed and the pellet was lysed in 100 μL (per million cells) of digitonin lysis buffer (75 mM NaCl, 1 mM NaH_2PO_4, 8 mM Na_2HPO_4, 250 mM sucrose, 200 μg/mL digitonin, and protease inhibitor cocktail) with gentle but thorough resuspension for 10 min. The lysate was centrifuged at 13,000 × *g* for 5 min at 4 μC. The resultant supernatant was collected as the cytosolic fraction. The pellet was then resuspended with a fresh volume of digitonin lysis buffer, sonicated for 5 s, and centrifuged at 13,000 × *g* for 5 min at 4 °C. The supernatant contained the mitochondria-enriched fraction. The purity of sub-cellular fractions was confirmed by immunoblotting with antisera to mitochondrially located VDAC or cytosolic glyceraldehyde 3-phosphate dehydrogenase (GAPDH) as described below.

2.7. Immunoblotting

All fractions collected were assayed for protein concentration using the BCA protein assay kit (Pierce Chemical Co., Rockford, IL). Each 30–50 μg of sample proteins were resolved by denaturing electrophoresis using 8–15% SDS-PAGE (Mini-PROTEAN II, Bio-Rad Laboratories, Hercules, CA) and transferred to nitrocellulose membranes for 1 h at 15 V using Trans-Blot SD Semi-Dry Transfer Cell (Bio-Rad). Immunodetection was by chemiluminescence (SuperSignal ULTRA, Pierce, Rockford, IL) using specific antibodies diluted in PBS with 0.05% (v/v) Tween 20 and 5% (w/v) powdered milk. Anti-HSP25, anti-HSP40, anti-HSP60, anti-HSP70i and anti-grp75 were from Stressgen (Victoria, BC); anti-HSP105 was from Santa Cruz and anti-GAPDH (1:2500) was made in-house [20]. Secondary anti-mouse and anti-rabbit horse-radish peroxidase conjugated secondary antibodies (Pierce) were used at 1:20,000 dilutions. All antibodies were used at 1:2,000 dilutions unless otherwise stated.

2.8. DEAE-sepharose column purification of HSP25

Cells were grown to confluence in 15 T150 dishes and treated with TFEC (6 h, 250 μm). Whole cells were washed in ice-cold PBS, harvested by scraping and pelleted in microcentrifuge tubes and lysed in 4.5 mL of buffer containing 20 mM Tris, 0.25 M sucrose, 1 μM dithiothreitol (DTT), and protease inhibitor cocktail (Roche, Switzerland) with sonication. The resulting lysates were centrifuged at 14,000 rpm for 15 min and supernatant was applied to a 2 cm × 10 cm column composed of diethylaminoethyl (DEAE)-sepharose fast-flow resin (Sigma), pre-equilibrated with buffer containing 20 mM Tris, 0.1 mM EDTA, 2 mM DTT and 0.1% CHAPS. After adding the sample, equilibration buffer was passed through with a continuous gradient from 0 to 1 M NaCl (total volume of 400 mL), maintained at a flow rate of 1 mL/min. Eighty fractions were collected (approx. 5 mL each). Every third fraction was screened for HSP25 by Western blot and the fraction with the highest concentration of the HSP25 was subjected to subsequent analysis.

2.9. In-gel digestion of HSP25 containing bands

DEAE-purified samples and HSP25 protein standard (Stressgen) were separated by SDS-PAGE on 4–15% gradient gel. Bands were visualized by silver staining, performed as described by manufacturer's protocol (Bio-Rad). Bands were excised and transferred to 1.5 mL microcentrifuge tubes. Method for in-gel digestion was adopted and modified from established protocol described previously [21]. The gels were rinsed three times with a destaining solution containing 6 mM potassium ferricyanide. They were then taken through two hydration/dehydration cycles with 50 mM ammonium bicarbonate and acetonitrile, respectively. All washing steps were performed with 10 min vortexing using 1 mL of the stated solvent. Next, the dried gel was incubated in 100 μL of 10 mM

DTT for 1 h at 60 °C. DTT solution was removed and replaced with 100 μL of 55 mM iodoacetamide in 50 mM ammonium bicarbonate and incubated at room temperature for 45 min. Iodoacetamide solution was removed and gels were washed with another hydration/dehydration cycle. The gels were dried again and cold trypsin (25 ng/μL in 50 mM ammonium bicarbonate) was added, followed by 45 min of incubation on ice. Thereafter, the digestion solution was removed and 30 μL of 25 mM ammonium bicarbonate was added. Tryptic digestion was allowed to proceed overnight at 37 °C with subsequent sonication for 20 min and the resultant aqueous liquid harvested and spiked with 0.1% trifluoroacetic acid for QTOF-MS analysis.

2.10. Mass spectrometric analysis

Peptide digests were analyzed by on-line nano-LC/ESI MS/MS using a QTOF mass spectrometer equipped with a CapLC system (Waters, Milford, MA). The stream select module was configured with a 5 mm × 300 μm i.d. trap column packed with 5 μm C particles (LC Packings, San Francisco, CA) connected by a ZU1XC metallic union (Valco, Houston, TX) to a 20 cm × 75 μm i.d. nanoscale analytical column pack in-house with 5 μm Jupiter C18 particles (Phenomenex, Torrance, CA) using the method described previously (Kennedy and Jorgenson, 1989). Peptide samples were injected onto the trap column at 10 μL/min, cleaned-up and back-flushed to the analytical column at 0.5 μL/min using gradient elution. Binary gradients of 5–60% solvent B were generated over 30 min, followed by 60% B for 5 min and 60–90% B for 5 min (solvent A: 3.3% acetonitrile, 1.7% isopropanol and 0.1% trifluoroacetic acid; solvent B: 63.3% acetonitrile, 31.7% isopropanol and 0.1% trifluoroacetic acid). QTOF parameters were set as follows: electrospray potential, 3.6 KV; cone voltage, 35 V; extraction cone, 0 V; and source temperature, 100 °C. The instrument was operated at a mass resolving power of 6000. For MS/MS, the scan time was set to 2 s, the precursor isolation width set to 4 Da, and the collision energy set to 25–45 eV according to the *m*/*z* of the precursor and the charge state.

2.11. HSP25 silencing by siRNA

Cells were grown on six-well plates to 60–70% confluence before transfection with siRNA (small interfering RNAs). Custom-made siRNA designed for silencing *HSP25* (accession number: NM_013560) expression was obtained from Santa Cruz. Various volumes (4–8 μL) of 10 μM siRNA were added to 80 μL of transfection medium (OptiMEM, Invitrogen) and incubated at room temperature for 5 min. Separately, transfection reagent (4–8 μL; Dharmafect4, Dharmacon, Chicago, IL) was incubated with transfection medium (80 μL) for the same duration. The two tubes were mixed gently and incubated at room temperature for 20 min. Following this incubation period, TAMH cells were washed with transfection medium alone. A 640 μL of transfection medium were added to the siRNA/transfection reagent mix and the entire volume was added onto the cells. After incubation at 37 °C for 6 h, 800 μL of normal growth medium (DMEM/F12) was added to each well. Incubation was continued for 24 h, and thereafter medium was replaced with fresh growth medium and cells were incubated for another 24 h. Cells were harvested by trypsinization and subjected to immunoblot analysis for evaluation of transfection efficiency. Cells with an optimum siRNA/transfection reagent ratio for gene silencing were treated with TFEC. TFEC was administered 30 h after the initial transfection. A scrambled siRNA sequence was used as a negative control (Ambion, Austin, TX).

2.12. Viability assay by MTT

Cells were seeded and grown to confluence on 96-well plates. After TFEC treatment, the MTT assay was performed as previously described [16,22]. For heat shock experiments, 96-well plates were suspended in a shaking water bath maintained at 43 °C for 1 h. TFEC was administered 12 h after the initial heat shock.

3. Results

3.1. Microarray analysis of TFEC treated TAMH cells

To assess genomic responses to TFEC-induced intramitochondrial damage, microarray analysis was performed on TFEC-treated TAMH cells over a period of 2–6 h. A total of 67, 179 and 303 genes were differentially regulated (>2-fold or <0.5-fold) at 2, 4 and 6 h, respectively (Table 1). Briefly, a large number of genes relating to homeostatic stress response, apoptosis, metabolism, transporters and transcriptional regulation were upregulated, while genes associated with cell cycling and immune response were down-regulated after TFEC treatment (Supplementary data, Table S1).

Among the early stress responses detected, the most significant were upregulation of a number of genes belonging to the heat shock protein superfamily. More than two-fold increases were observed for *HSP70i* (denoted as HSP68 and HSP68A on the array), *HSP40* (*HSP40B1* and *HSP40B9*), *HSP25*, *HSP86* and *HSP105* 4 h after treatment with TFEC (Fig. 1). The most highly upregulated gene was *HSP70i*, whose expression increased by 19.6- and 35.7-fold at 4 and 6 h, respectively. Microsomal heme oxygenase-1 (HO-1) also demonstrated a dramatic induction of 17.2-, 29.4- and 31.0-fold versus control cells at 2, 4 and 6 h, respectively (Table 2). More importantly, this HSP regulation profile is unique to TFEC, as other known hepatotoxicants treated at concentrations that caused

Table 1 – Microarray analysis of TFEC treated TAMH cells

Treatment (h)	Two-fold increase	Two-fold decrease	Total
2	47	20	67
4	105	74	179
6	153	150	303

TAMH cells were treated with 200 mM TFEC for 2, 4, and 6 h. Gene expressions were normalized by their respective vehicle treated controls and displayed as a function of fold changes. Total number of genes significantly upregulated (at least two-fold greater than control) or down-regulated (at least two-fold lesser than control) at respective time points are tabulated as shown.

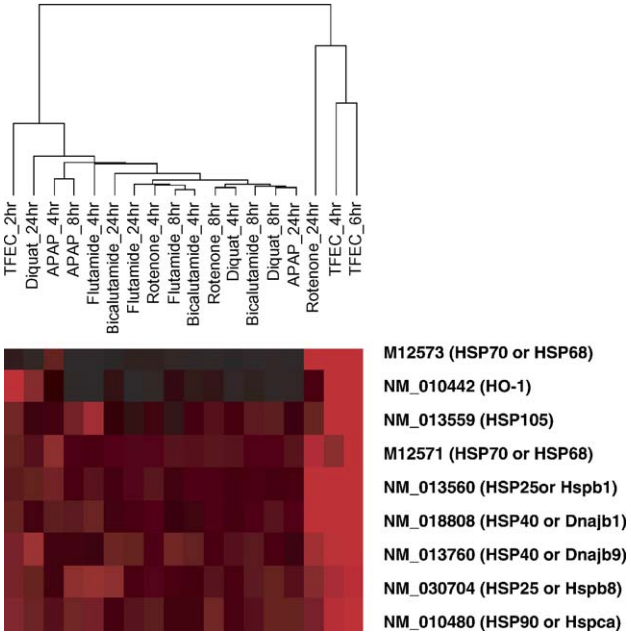

Fig. 1 – Heat-map display of the eight TFEC-inducible *HSP*s. Genes with >two-fold upregulation are shaded in red. Intensity of the shading is proportional to the magnitude of mRNA induction. Responses were compared with other known hepatotoxicant treatments including rotenone (1 μM), acetaminophen (5 mM), diquat (20 μM) and flutamide (75 μM) dosed for 4, 8 and 24 h. The expression profiles were compared and clustered by similarity using the GeneSifter software. Red shading denotes upregulation, green shading denotes down regulation and black shading denotes genes with no significant change in expression level.

approximately the same extent of lethality in TAMH cells (including acetaminophen, rotenone, diquat and flutamide) do not yield a similar pattern (Fig. 1). As shown in the heat-map of nine representative *hsp* gene expression profiles, TFEC (4 and 6 h) treated cells clustered closely together (Fig. 1).

Table 2 – Microarray analyses of de novo TFEC-inducible hsp genes

Gene name	Fold induction		
	2 h	4 h	6 h
HSP68 (or HSP70i)	1.7	19.6	35.7
Heme oxygenase-1	17.2	29.4	31.0
HSP 105	1.3	3.5	4.8
HSP25	1.4	3.4	4.7
HSP68A	1.3	1.9	4.6
HSP40B1	1.2	3.2	4.1
HSP40B9	1.9	3.2	4.0
HSP86	1.3	2.0	2.5

Analyses were performed on TAMH cultures treated with 200 μM TFEC for 2, 4 or 6 h. Results have been expressed as a normalized ratio of the gene expression in the TFEC-treated samples against aqueous vehicle treated controls. Selected highly expressed *HSP* genes are listed according to fold induction at 6 h.

3.2. *Quantitative RT-PCR analysis of heat shock proteins*

To validate the upregulation of *hsp* transcripts identified from microarray experiments, quantitative real-time PCR was performed on selected HSPs. As clearly demonstrated in Fig. 2, we have confirmed the transcriptional upregulation of *HO-1* (or *HSP32*), *HSP70i*, *HSP25*, *HSP40* and *HSP105*. In contrast, mitochondrial *HSP60* and *mtHSP70* both showed a lack of induction at any of the time points examined (they were also not upregulated from microarray results).

3.3. *Immunoblot analysis of heat shock protein expression*

Confirmatory Western blots were also performed to determine if increased protein expression paralleled transcriptional upregulation. Accordingly, TAMH cells were treated with 250 μM TFEC and total cell lysates were probed with specific antibodies/antisera to heat shock proteins of interest using standard procedures as described in Section 2. We observed a significant upregulation of HSP70i from 2 to 8 h (Fig. 3). Microsomal HO-1 also showed a time-dependent induction. However, levels of HSP40 and HSP105 did not show any significant increase despite obvious transcriptional changes. Other ER-bound and mitochondrial HSPs did not manifest TFEC-dependent induction. Interestingly, a novel immunoreactive band against HSP25 was observed that was inducible after continued incubation with TFEC. This protein had a molecular weight of approximately 50 kDa, suggestive of a dimer of HSP25. Furthermore, it was non-dissociable, even under an extreme denaturing and reducing environment using high concentrations of DTT (up to 500 mM) and β-mercaptoethanol (up to 2 M) (Fig. 4A). When cell lysates were partially purified with DEAE-sepharose column, the 50 kDa band became more sensitive to DTT (100 and 200 mM) and Tris(2-carboxyethyl)phosphine (TCEP; 1 and 10 mM) reducing conditions. At 10 mM TCEP, the band completely dissociated into its monomer units at 25 kDa (Fig. 4B). The subcellular localization of HSP25 was determined by probing cytosolic and mitochondrial fractions of TAMH cells treated for 0, 4 and 8 h with TFEC. As shown in Fig. 4C, the 25 kDa immunoreactive band decreased in the cytosol with a corresponding increase in the mitochondria after 4 and 8 h. The higher molecular weight bands were only apparent after treatment with TFEC, and were localized in both compartments. However, the apparent dimer decreased in the cytosol with a concomitant increase in mitochondria over time (Fig. 4C).

Separately, DEAE-purified apparent dimer and monomer of HSP25 were separated by gel electrophoresis and excised for in-gel digestion. They were then analyzed by ESI-QTOF mass spectrometry and compared against a recombinant protein standard. Twelve signature peptides were identified from the protein standard. At least five of the peptide masses were correspondingly observed in the apparent dimer and monomer (Supplementary data, Fig. S1).

3.4. *HSP25 silencing by siRNA*

In order to provide further evidence for the formation of an HSP25 dimer, the gene was silenced by siRNA. Effective gene silencing was achieved with 4 μL of siRNA (10 mM) plus 6 μL of

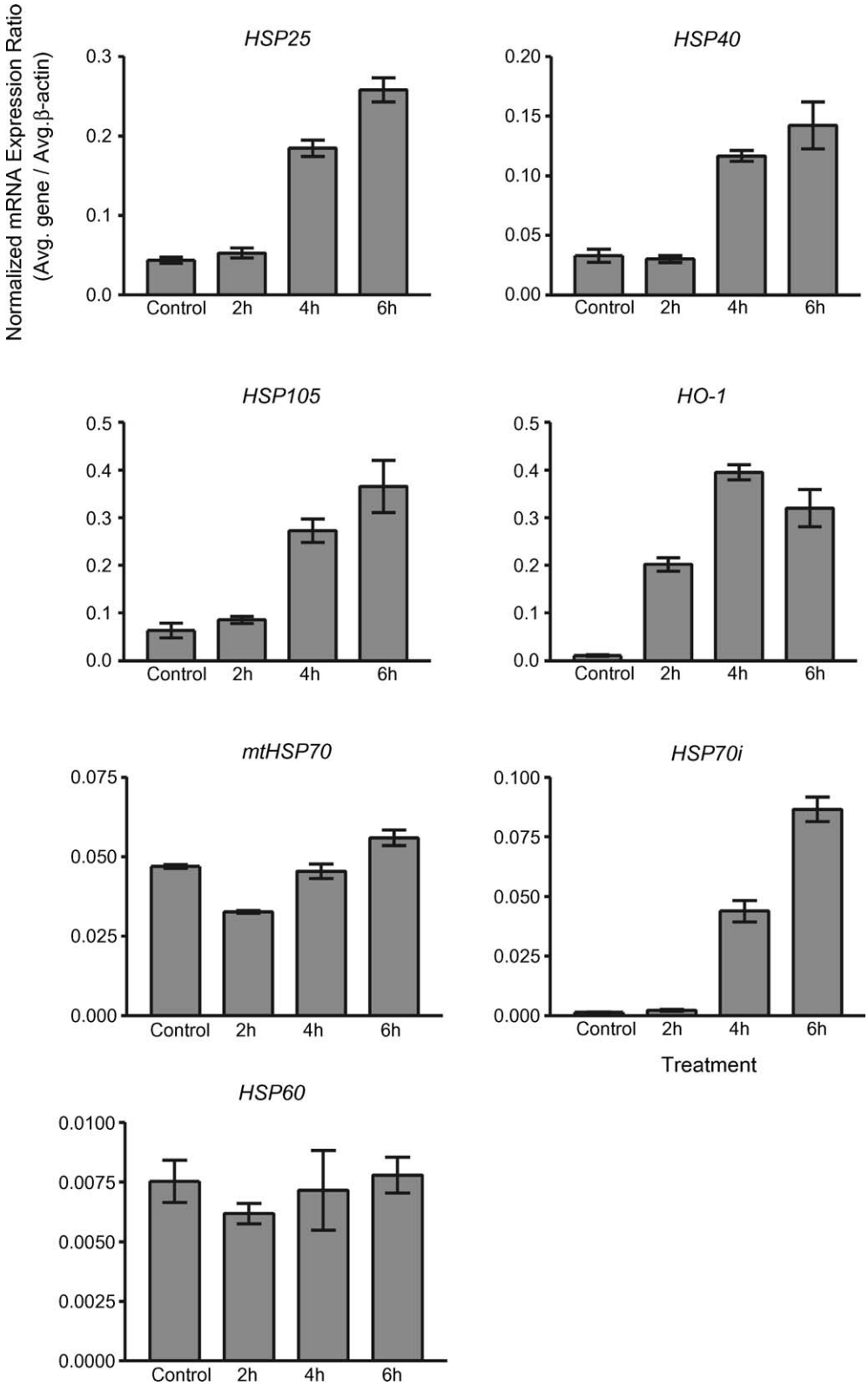

Fig. 2 – Real time quantitative RT-PCR for selected genes. Genes were validated with real-time quantitative RT-PCR using SYBR Green fluorogenic probes. Results are expressed as a normalized ratio using the housekeeping gene GAPDH as reference. Each profile is displayed as a separate graph including *HSP25*, *HSP40*, *HSP70*i, *mtHSP70*, *HSP60*, *HSP 105* and *HO-1*. Each data point is the taken as the average of three replicates with SEM displayed as the *y*-error bars.

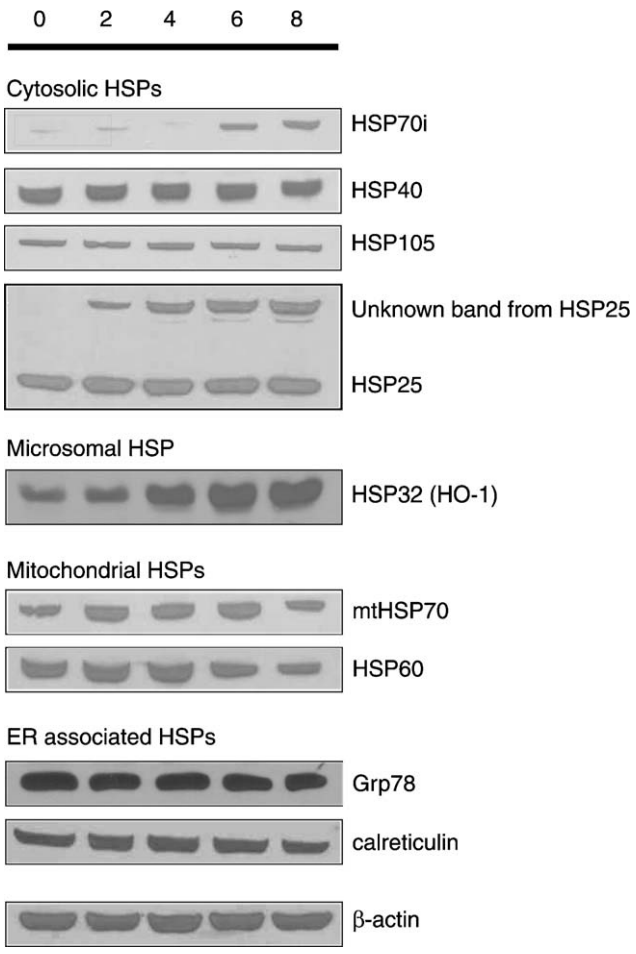

Fig. 3 – Immunoblot assay for various HSPs following TFEC (250 μM) treatment of TAMH cells. TAMH cells were treated with 250 μM TFEC for 0, 2, 4, 6 and 8 h. Total cell lysates were blotted with polyclonal anti-HSP25, anti-HSP40, anti-HSP60, anti-HSP70i, anti-HO-1, anti-mtHSP70, anti-HSP105, anti-grp78 and anti-calreticulin. Loading control was anti-β-actin.

transfection reagent for each well in a six-well dish. The efficiency of the silencing was approximately 85% at 48 h after initial transfection (Fig. 5A). Transfected cells were subsequently treated with TFEC for 8 h (250 μM). HSP25 protein expression was reduced to about 25% of control. Likewise, the expression of the apparent dimer was reduced to 20% of control, with little change in expression level of HSP25 in either untransfected or scrambled siRNA transfected cells (Fig. 5B).

3.5. *Heat shock pretreatment of TAMH cells*

The functional significance of an apparently coordinated upregulation of heat shock proteins was evaluated using a "gain-of-function" approach. A mild heat shock pretreatment can be used to non-selectively induce HSP without causing lethality in host cells, a phenomenon also known as heat shock preconditioning [23–25]. Since HSP response is cell-type dependent, the heat shock response in TAMH cultured cells was examined using an initial 43 °C/30 min incubation, and HSP expression at various timepoints after the initiation of the temperature shock was then assessed by Western blot analysis. As shown in Fig. 6, HSP70i, HSP40, HSP25 and HSP105 were all upregulated between 4 and 16 h after heat shock pretreatment. The mitochondrial levels of HSPs including mtHSP70 (a.k.a. GRP75) and HSP60 were mildly upregulated relative to cytosolic HSP responses. In separate experiments, the expressions of these HSPs were optimized by changing the duration of heat shock (15 min to 3 h) as well as varying the temperature (37–45 °C) (data not shown). These results helped us establish the optimum conditions for heat shock in TAMH cells at 42–43 °C for 30–60 min, and the maximum induction of HSPs occurred between 4 and 16 h after the initial heat shock.

3.6. *Cytoprotective effect of heat shock pretreatment on TFEC-induced toxicity*

TAMH cells were incubated with TFEC (250 μM) for 0–12 h after an initial heat shock treatment. Cellular viability was assessed using MTT assay. Results demonstrated a significant increase in viability of TAMH cells at 8 and 12 h after TFEC treatment ($P < 0.05$). Cells treated with higher doses of TFEC (500 μM) showed improved survival after heat shock, although a complete reversal to control cell viability was not apparent (Fig. 7).

4. Discussion

In this study, TFEC was used to induce mitochondrially directed subcellular damage in an attempt to investigate the early genomic responses to dysfunction at the level of this organelle. Microarray analysis of TAMH cells treated with TFEC showed time-dependent increases in gene expression over the first 6 h. Apart from genes known to inhibit cell cycling, signal transduction, transcriptional regulation and metabolism, TFEC demonstrated a robust induction of heat shock proteins that was different from what has been observed following incubation of TAMH cells with other cytotoxicants. This result is consistent with the hypothesis that heat shock responses are an important cellular defense mechanism in the face of intramitochondrial dysfunction [26].

Heat shock proteins are now recognized as a superfamily of highly inducible stress proteins that are responsive to a broad range of endogenous and exogenous cell stressors [23–25]. Most HSPs have well-defined subcellular localization(s). For example, HSP60 is predominantly mitochondrial, HSP70i is cytosolic and GRP78 is ER-bound. A generalized, but not exclusive role, for heat shock proteins is to bind exposed hydrophobic regions of unfolded, misfolded or modified proteins in order to help attain/restore biological function [23].

TFEC treatment of TAMH cells resulted in dramatic induction of *HSP70i*, *HO-1*, *HSP40*, *HSP25* and *HSP105* transcripts within the first 4 h of treatment as confirmed by both microarray and RT-PCR. Corresponding increases in protein expression were also observed for HSP70i and HO-1 over the first 8 h. Although we did not observe commensurate evidence of protein upregulation for HSPs other than HSP70i and HO-1

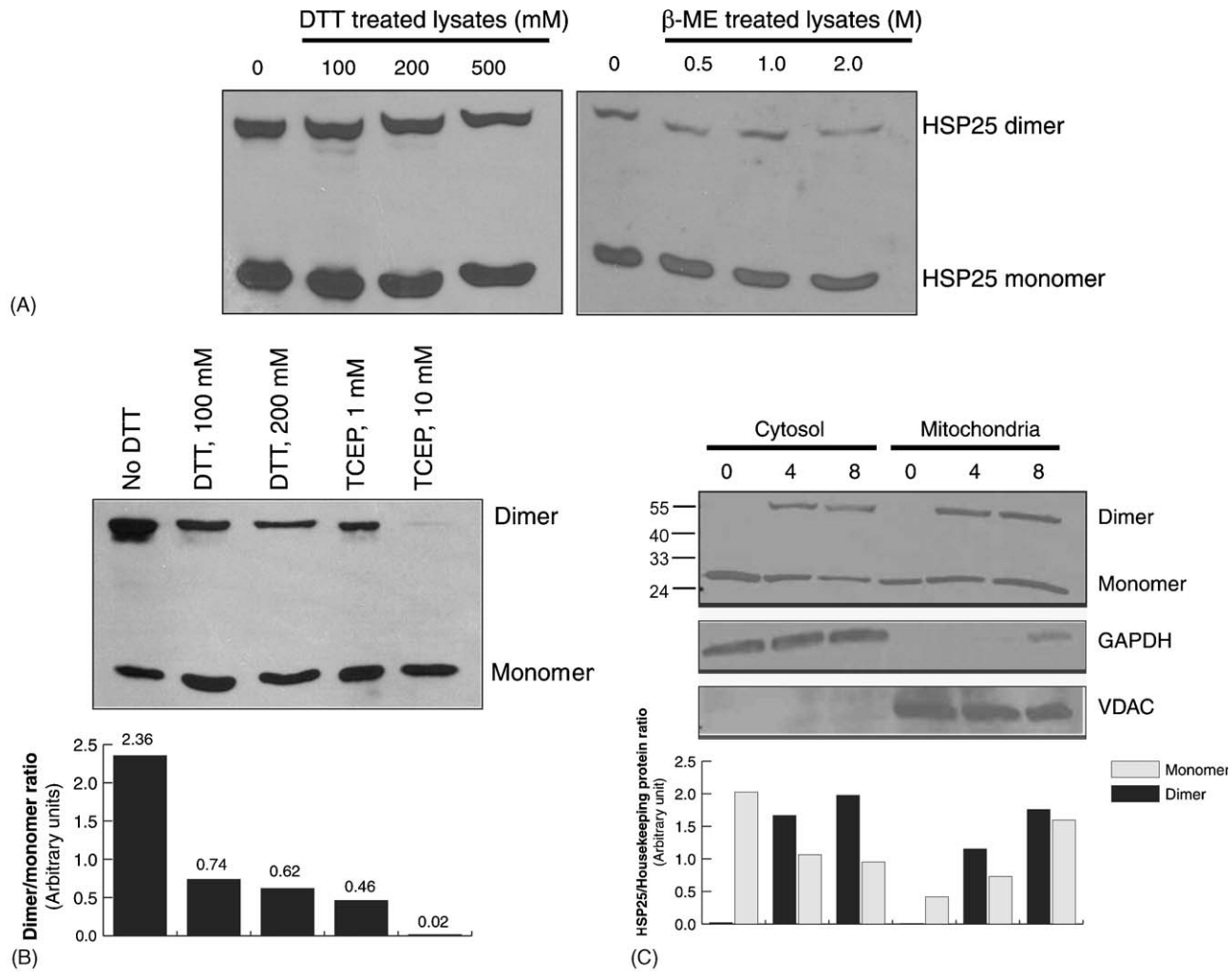

Fig. 4 – Immunoblot assays characterizing the apparent dimer of HSP25. (A) TAMH cells treated with TFEC (250 μM) for 6 h were incubated with different concentrations of DTT (100, 250, 500 mM) and β-mercaptoethanol (0.5, 1, 2 M) before SDS-PAGE and Western blot analysis with polyclonal anti-HSP25. (B) Samples of TAMH cells treated with TFEC (6 h, 250 μM) were purified on a DEAE-sepharose column. The fraction positive for HSP25 was applied for DTT (100 and 200 mM) and TCEP (1 and 10 mM) incubations (20 min at 95 °C) before SDS-PAGE and Western blot analysis with polyclonal anti-HSP25. (C) TAMH cells were subsequently treated with TFEC for 0, 4 and 8 h. Mitochondrial and cytosolic fractions were blotted with polyclonal anti-HSP25. Polyclonal anti-GAPDH and anti-VDAC were used as loading controls for cytosol and mitochondria, respectively. Intensity of each HSP25 band is quantified by densitometry and displayed as a graph below the blot.

by Western blot analyses, this could suggest a delayed translational effect in comparison to HSP70i and HO-1. Alternatively, the existence of multi-modal signaling pathways in the regulation of specific HSP isoforms is a possibility. Somewhat surprising was the observation that cytosolic HSPs (with the exception of the microsomal HO-1) were the most highly upregulated, even though TFEC damage originates from within the mitochondrial matrix. While other ER and mitochondrial HSPs are known to be inducible after other kinds of stress [27,28], TFEC did not demonstrate similar responses. The expression profile was also different from the pattern commonly observed after a mild temperature shock, where HSP60 and HSP105 are significantly upregulated (Fig. 6).

The underlying significance of this unanticipated cytosolic HSP response is not clear. However, it can be assumed that there is an early signaling event from the otherwise compartmentalized mitochondria that is directed towards the cytosol (as well as other subcellular compartments) where transcription factors become activated, leading to the induction of cytosolic stress proteins. We have previously reported evidence for such events with the demonstration that the cytosolic ''cap-and-collar'' transcription factor, Nrf2, is rapidly activated (within 1 h) after TFEC treatment to mediate an antioxidant response [15]. Induction of another stress-responsive transcription factor, ATF3, also supports the conclusion that ER-driven transcriptional changes are a direct consequence of intramitochondrial damage [15]. Hence, early mitochondrial injury rapidly generates secondary responses that affect the rest of the cell.

Accordingly, further experiments were carried out to determine if the specific induction of cytosolic HSPs confers protection from TFEC damage. Mild heat shock pretreatment

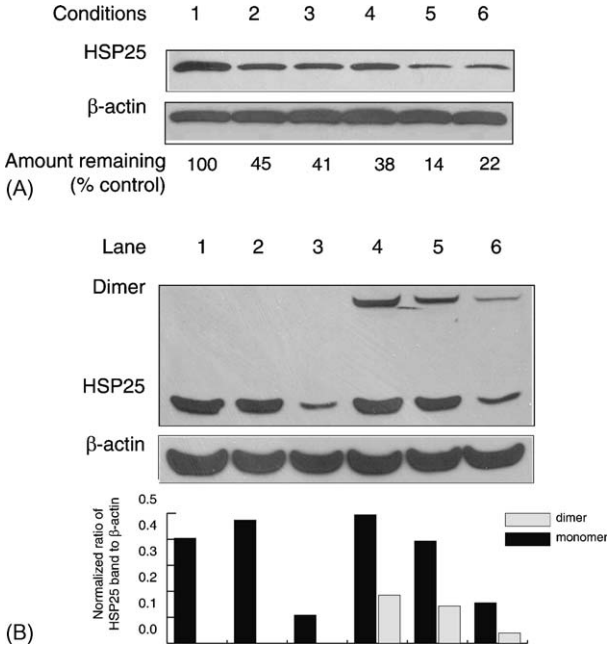

Fig. 5 – Silencing of *HSP25* by siRNA. (A) TAMH cells were transfected with different ratios of siRNA-to-transfection reagent for 48 h. These conditions were: (1) untransfected control; (2) 4 μL siRNA, 4 μL transfection reagent; (3) 6 μL siRNA, 4 μL transfection reagent; (4) 8 μL siRNA, 4 μL transfection reagent; (5) 4 μL siRNA, 6 μL transfection reagent; (6) 4 μL siRNA, 8 μL transfection reagent. HSP25 protein expression was monitored by immunoblot assay using specific polyclonal anti-HSP25 antibodies. HSP25 protein levels are expressed as a normalized ratio of the respective β-actin levels. (B) TAMH cells were transfected with condition 5 as described earlier. At 30 h post-transfection, TFEC (250 μM) was administered and immunoblot assay was performed on cell lysates that were subjected to 8 h treatment with TFEC. Lanes 1 and 4 are untransfected cells, lanes 2 and 5 are cells transfected with the negative control siRNA, and lanes 3 and 6 are transfected with HSP25 siRNA. Lane 1–3 are untreated cells and lanes 4–6 are cells treated with TFEC. The relative protein levels and HSP25 monomer and the apparent dimer are expressed as a normalized ratio of the β-actin loading control.

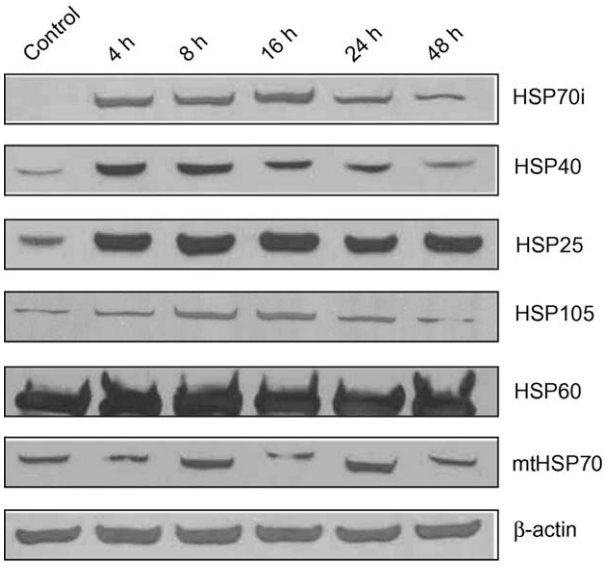

Fig. 6 – Immunoblot assay for various HSPs after heat shock pretreatment of TAMH cells. TAMH cells were shocked at 43 °C for 30 min and replaced into the 37 °C CO_2 incubator before they were harvested at 4, 8, 16, 24 and 48 h. They were blotted with a representative list of HSPs including HSP25, HSP40, HSP60, HSP70i, mtHSP70 and HSP105. The loading control was β-actin.

caused upregulation of several HSPs in TAMH cells and was found to improve cell viability after TFEC treatment. However, a complete reversal of TFEC toxicity by pre-emptive HSP induction was not observed, most likely because the HSPs induced did not reside in the mitochondria. Since the majority of the mitochondrial proteins are synthesized in the cytoplasm and then transported into the mitochondria in an unfolded state, where mitochondria-accessible chaperones (including HSP60 and HSP10) mediate folding and maturation [28], it is unlikely that elevations in cytosolic HSPs can significantly repair existing mitochondrial protein lesions. Nonetheless, elevations in cytosolic HSPs may play some role in preventing the progression of cellular injury. Partial protection against TFEC-induced renal injury in rats through amphetamine pretreatment (a pharmacological method to mimic heat shock preconditioning) was recently reported and prior ER stress induction provided even more pronounced protection [29]. Evidence for ER stress induction was not found

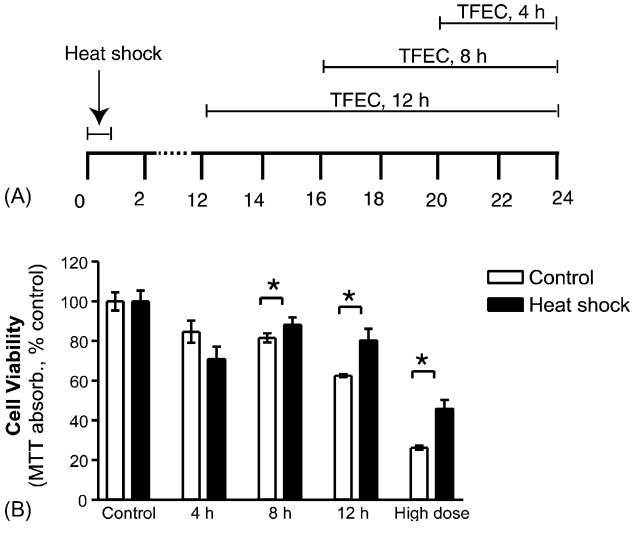

Fig. 7 – MTT viability assay of heat shocked TAMH cells after various durations of TFEC (250 μM) treatment. (A) Cells were heat shocked at 43 °C for 1 h, pre-incubated for another 11, 15, 19 h and treated for 12, 8 and 4 h, respectively. (B) Viability was measured by MTT assay. Results are expressed as a percentage of viable cells in the untreated controls with ±S.D. ($n = 6$) (asterisk (*) denotes a statistically significant difference between control and heat shock cells with $p < 0.05$).

in the present studies and the discrepancy may be due either to differences in the models used or differences in time-course responses.

The partial HSP-mediated cytoprotection observed in these studies may result from several factors. For example, there is evidence that nonspecific hydrophobic interactions of HSP70i (the major HSP induced during heat shock) with other proteins may have effects beyond restoration of protein damage. The promiscuity of HSPs binding to various proteins likely participates in modulating other cell signaling events including those related to apoptosis [30]. Previous studies have provided evidence for HSP70i-mediated inhibition of JNK [31]. Other studies have demonstrated binding of HSP70i to Apaf1, thus inhibiting the formation of the apoptosome and subsequent activation of caspases [32]. Similarly, HSP70 association with AIF blocks apoptosis, as well as interference with the balance between BAX/BCL-2 both of which favor cellular survival [33–35].

Another interesting result from our investigation was the observation of a 50 kDa immunoreactive protein towards HSP25 antibody after TFEC treatment. This band was responsive to specific HSP25 silencing by siRNA, and produced multiple peptide masses that matched exactly those derived from protein standard, thus indicating that it is most likely a HSP25 dimer. It has been independently reported that under highly oxidative conditions, native HSP25 can form a dimer through a disulfide bridge [36]. Further studies led to the suggestion that this HSP25 dimer played a functional role in maintaining cellular thiol status. HSP25 is also known to interact with GSH/GSSG to preserve oxidative balance [36,37]. More recently, substitution of Cys141 by alanine in murine HSP25 was found to inhibit dimer formation and decrease the cytoprotective activity of the protein after hydrogen peroxide treatment [38]. This mechanism is even more attractive, given the high inducibility and cellular abundance of HSP25 following stress events [39]. However, from the studies reported here, the situation is more complex. Contrary to earlier reports, we have observed that the putative HSP25 dimer formed in TAMH cells after TFEC treatment is resistant to standard protein denaturing and reducing environments [38]. It was nonetheless dissociable when a partially purified sample was applied to extreme reducing conditions (10 mM TCEP). This finding suggests that the dimer was likely held together by strong disulfide bonds that were either well-protected by neighboring peptides, and/or have undergone further structural modification that rendered the dimer resistant to reduction with DTT or β-mercaptoethanol. Although mass spectrometric analysis of this dimer confirmed its identity, further MS experiments will be necessary to fully characterize the structure.

Furthermore, there appears to be two separate pools of HSP25, i.e. cytosolic and mitochondrial. Cytosol-to-mitochondria subcellular relocalization of HSP25 after treatment with TFEC suggests that there is some pathophysiological role for HSP25 in the mitochondria. In recent years, studies have described HSP25 relocalization and cytoprotective roles within the mitochondria in various cell lines [40–42]. For example, its was demonstrated that mitochondrial HSP25 can block mitochondrial cytochrome *c* release and inhibit apoptosis [42]. Independently, the suppression of the mitochondrial permeability transition by HSP25 was observed [41]. Therefore, it is reasonable to hypothesize that the mitochondrial accumulation of HSP25 could constitute an important cellular response to limit the progression of mitochondrial injury after TFEC treatment.

Overall, this study provides persuasive evidence for preferential cytosolic HSPs upregulation in response to specific intramitochondrial damage mediated by TFEC. While the signaling events linking the mitochondrial lesions to cytosolic responses are not well understood, this form of stress protein induction may play a role in limiting the progression of chemically induced cellular injury.

Acknowledgements

This work was supported by NIH Grants GM32165 (SDN), CA74131 (NF), UW NIEHS sponsored Center for Ecogenetics and Environmental Health: NIEHS P30ES07033 and Pfizer Inc.

Appendix A. Supplementary data

Supplementary data associated with this article can be found, in the online version, at doi:10.1016/j.bcp.2006.03.019.

REFERENCES

[1] Halestrap AP, Doran E, Gillespie JP, O'Toole A. Mitochondria and cell death. Biochem Soc Trans 2000;28:170–7.
[2] Hengartner MO. The biochemistry of apoptosis. Nature 2000;407:770–6.
[3] Duchen MR. Roles of mitochondria in health and disease. Diabetes 2004;53:S96–102.
[4] Krahenbuhl S. Mitochondria: important target for drug toxicity? J Hepatol 2001;34:334–6.
[5] Anders MW, Dekant W. Glutathione-dependent bioactivation of haloalkenes. Annu Rev Pharmacol Toxicol 1998;38:501–37.
[6] IARC. Tetrafluoroethylene. IARC Monogr Eval Carcinog Risks Hum1999;71:1143. http://www-cie.iarc.fr/htdocs/monographs/vol71/048-tetrafluo.html.
[7] James EA, Gygi SP, Adams ML, Pierce RH, Fausto N, Aebersold RH, et al. Mitochondrial aconitase modification, functional inhibition, and evidence for a supramolecular complex of the TCA cycle by the renal toxicant S-(1,1,2,2-tetrafluoroethyl)-L-cysteine. Biochemistry 2002;41:6789–97.
[8] Keller DA, Kennedy Jr GL, Ross PE, Kelly DP, Elliott GS. Toxicity of tetrafluoroethylene and S-(1,1,2,2-tetrafluoroethyl)-L-cysteine in rats and mice. Toxicol Sci 2000;56:414–23.
[9] Lock EA, Ishmael J. The nephrotoxicity and hepatotoxicity of 1,1,2,2-tetrafluoroethyl-L-cysteine in the rat. Arch Toxicol 1998;72:347–54.
[10] Cooper AJ, Pinto JT. Aminotransferase, l-amino acid oxidase and beta-lyase reactions involving l-cysteine S-conjugates found in allium extracts relevance to biological activity? Biochem Pharmacol 2005;69:209–20.
[11] Odum J, Green T. The metabolism and nephrotoxicity of tetrafluoroethylene in the rat. Toxicol Appl Pharmacol 1984;76:306–18.

[12] Cooper AJ, Bruschi SA, Anders MW. Toxic, halogenated cysteine S-conjugates and targeting of mitochondrial enzymes of energy metabolism. Biochem Pharmacol 2002;64:553–64.
[13] Bruschi SA, West KA, Crabb JW, Gupta RS, Stevens JL. Mitochondrial HSP60 (P1 protein) and a HSP70-like protein (mortalin) are major targets for modification during S-(1,1,2,2-tetrafluoroethyl)-L-cysteine-induced nephrotoxicity. J Biol Chem 1993;268:23157–61.
[14] Wu JC, Merlino G, Cveklova K, Mosinger Jr B, Fausto N. Autonomous growth in serum-free medium and production of hepatocellular carcinomas by differentiated hepatocyte lines that overexpress transforming growth factor alpha 1. Cancer Res 1994;54:5964–73.
[15] Ho HK, White CC, Fernandez C, Fausto N, Kavanagh TJ, Nelson SD, et al. Nrf2 activation involves an oxidative-stress independent pathway in tetrafluoroethylcysteine-induced cytotoxicity. Toxicol Sci 2005;86: 354–64.
[16] Ho HK, Hu ZH, Tzung SP, Hockenbery DM, Fausto N, Nelson SD, et al. BCL-xL overexpression effectively protects against tetrafluoroethylcysteine-induced intramitochondrial damage and cell death. Biochem Pharmacol 2005;69:147–57.
[17] Pierce RH, Franklin CC, Campbell JS, Tonge RP, Chen W, Fausto N, et al. Cell culture model for acetaminophen-induced hepatocyte death in vivo. Biochem Pharmacol 2002;64:413–24.
[18] Bolstad BM, Irizarry RA, Astrand M, Speed TP. A comparison of normalization methods for high density oligonucleotide array data based on variance and bias. Bioinformatics 2003;19:185–93.
[19] Single B, Leist M, Nicotera P. Simultaneous release of adenylate kinase and cytochrome c in cell death. Cell Death Differ 1998;5:1001–3.
[20] Dietze EC, Schafer A, Omichinski JG, Nelson SD. Inactivation of glyceraldehyde-3-phosphate dehydrogenase by a reactive metabolite of acetaminophen and mass spectral characterization of an arylated active site peptide. Chem Res Toxicol 1997;10:1097–103.
[21] Shevchenko A, Wilm M, Vorm O, Mann M. Mass spectrometric sequencing of proteins silver-stained polyacrylamide gels. Anal Chem 1996;68:850–8.
[22] Plumb JA, Milroy R, Kaye SB. Effects of the pH dependence of 3-(4,5-dimethylthiazol-2-yl)-2,5-diphenyl-tetrazolium bromide-formazan absorption on chemosensitivity determined by a novel tetrazolium-based assay. Cancer Res 1989;49:4435–40.
[23] De Maio A. Heat shock proteins: facts, thoughts, and dreams. Shock 1999;11:1–12.
[24] Kregel KC. Heat shock proteins: modifying factors in physiological stress responses and acquired thermotolerance. J Appl Physiol 2002;92:2177–86.
[25] Ritossa F. Discovery of the heat shock response. Cell Stress Chaperones 1996;1:97–8.
[26] Sammut IA, Harrison JC. Cardiac mitochondrial complex activity is enhanced by heat shock proteins. Clin Exp Pharmacol Physiol 2003;30:110–5.
[27] Maniratanachote R, Minami K, Katoh M, Nakajima M, Yokoi T. Chaperone proteins involved in troglitazone-induced toxicity in human hepatoma cell lines. Toxicol Sci 2005;83:293–302.
[28] Schafler AE, Kirmanoglou K, Pecher P, Hannekum A, Schumacher B. Overexpression of heat shock protein 60/10 in myocardium of patients with chronic atrial fibrillation. Ann Thorac Surg 2002;74:767–70.
[29] Asmellash S, Stevens JL, Ichimura T. Modulating the endoplasmic reticulum stress response with trans-4,5-dihydroxy-1,2-dithiane prevents chemically induced renal injury in vivo. Toxicol Sci 2005;88:576–84.
[30] Garrido C, Gurbuxani S, Ravagnan L, Kroemer G. Heat shock proteins: endogenous modulators of apoptotic cell death. Biochem Biophys Res Commun 2001;286:433–42.
[31] Mosser DD, Caron AW, Bourget L, Denis-Larose C, Massie B. Role of the human heat shock protein hsp70 in protection against stress-induced apoptosis. Mol Cell Biol 1997;17:5317–27.
[32] Beere HM, Wolf BB, Cain K, Mosser DD, Mahboubi A, Kuwana T, et al. Heat-shock protein 70 inhibits apoptosis by preventing recruitment of procaspase-9 to the Apaf-1 apoptosome. Nat Cell Biol 2000;2:469–75.
[33] Gotoh T, Terada K, Oyadomari S, Mori M. hsp70-DnaJ chaperone pair prevents nitric oxide- and CHOP-induced apoptosis by inhibiting translocation of Bax to mitochondria. Cell Death Differ 2004;11:390–402.
[34] Ravagnan L, Roumier T, Kroemer G. Mitochondria, the killer organelles and their weapons. J Cell Physiol 2002;192:131–7.
[35] Zhou H, Kato A, Yasuda H, Odamaki M, Itoh H, Hishida A. The induction of heat shock protein-72 attenuates cisplatin-induced acute renal failure in rats. Pflugers Arch 2003;446:116–24.
[36] Zavialov AV, Gaestel M, Korpela T, Zav'yalov VP. Thiol/disulfide exchange between small heat shock protein 25 and glutathione. Biochim Biophys Acta 1998;1388:123–32.
[37] Arrigo AP. Hsp27: novel regulator of intracellular redox state. IUBMB Life 2001;52:303–7.
[38] Diaz-Latoud C, Buache E, Javouhey E, Arrigo AP. Substitution of the unique cysteine residue of murine Hsp25 interferes with the protective activity of this stress protein through inhibition of dimer formation. Antioxid Redox Signal 2005;7:436–45.
[39] Ehrnsperger M. Molecular chaperones in the life cycle of proteins New York: Marcel Dekker; 1997.
[40] Downs CA, Jones LR, Heckathorn SA. Evidence for a novel set of small heat-shock proteins that associates with the mitochondria of murine PC12 cells and protects NADH:ubiquinone oxidoreductase from heat and oxidative stress. Arch Biochem Biophys 1999;365:344–50.
[41] He L, Lemasters JJ. Heat shock suppresses the permeability transition in rat liver mitochondria. J Biol Chem 2003;278:16755–60.
[42] Samali A, Robertson JD, Peterson E, Manero F, van Zeijl L, Paul C, et al. Hsp27 protects mitochondria of thermotolerant cells against apoptotic stimuli. Cell Stress Chaperones 2001;6:49–58.